A COMPREHENSIVE MODEL FOR THE FATIGUE ANALYSIS OF FLEXIBLE PAVEMENTS CONSIDERING THE EFFECTS OF DYNAMIC AXLE LOADS

Fermín Navarrina, Corresponding Author
School of Civil Engineering — University of A Coruña
Escuela Técnica Superior de Ingenieros de Caminos, Canales y Puertos
Campus de Elviña, 15192 A Coruña, Spain
Tel: +34-981-167-000-1-1413; Fax: +34-981-167-170; Email: fermin.navarrina@udc.es
Webpage: http://caminos.udc.es/gmni

Luis Ramírez
School of Civil Engineering — University of A Coruña
Escuela Técnica Superior de Ingenieros de Caminos, Canales y Puertos
Campus de Elviña, 15192 A Coruña, Spain
Tel: +34-981-167-000-1-5475; Fax: +34-981-167-170; Email: luis.ramirez@udc.es

José París
School of Civil Engineering — University of A Coruña
Escuela Técnica Superior de Ingenieros de Caminos, Canales y Puertos
Campus de Elviña, 15192 A Coruña, Spain
Tel: +34-981-167-000-1-1414; Fax: +34-981-167-170; Email: jose.paris@udc.es

Xesús Nogueira
School of Civil Engineering — University of A Coruña
Escuela Técnica Superior de Ingenieros de Caminos, Canales y Puertos
Campus de Elviña, 15192 A Coruña, Spain
Tel: +34-981-167-000-1-1414; Fax: +34-981-167-170; Email: xesus.nogueira@udc.es

Manuel Casteleiro
School of Civil Engineering — University of A Coruña
Escuela Técnica Superior de Ingenieros de Caminos, Canales y Puertos
Campus de Elviña, 15192 A Coruña, Spain
Tel: +34-981-167-000-1420; Fax: +34-981-167-170; Email: manuel.casteleiro@udc.es

José Ramón Fernández-de-Mesa
Holding Eurovía España
San Martín de Guillar — Otero de Rey
27080 LUGO, Spain
Tel: +34-982-200-920; Fax: +34-982-201-116; Email: joseramon.fernandez@ovisa.es

6,235 words text + 4 figures × 250 words (each) + 1 tables × 250 words (each) = 7,485 words

November 14, 2014

ABSTRACT

A comprehensive model for the fatigue analysis of flexible pavements considering the effects of dynamic axle loads is presented in this paper. The main objective of this work is to quantify the reduction in the structural service life of the pavement due to the rise of the dynamic axle loads exerted by the traffic, as the progressive deterioration of the road profile occurs.

First, the procedure for the fatigue analysis of flexible pavements, as defined in the Spanish Standard 6.1–IC, is explained in detail. The implementation herein presented is specific for this Standard, but the underlying concepts are not restrictive, and the model can be easily adapted to fit the distinctive features of other regulations. Second, the concepts of accumulated damage and structural service life are formalized in mathematical terms. Next, dynamic axle loads are introduced, which leads to the definition of a suitable accumulated fatigue damage indicator that takes into account these effects. Dynamic axle loads are introduced in this formulation by means of a so-called effective dynamic load amplification factor. For the quantification of this factor, the Quarter-Car model is extended to allow for computing the time evolution of the dynamic axle load exerted by a heavy vehicle on the pavement. Finally, the model is completed by adding a simple procedure for simulating how the road profile deteriorates over time.

Finally, an application example is presented.

Keywords: flexible pavement design, dynamic axle load, accumulated damage indicator, pavement structural service life, Quarter-Vehicle model, IRI, road profile deterioration.

INTRODUCTION

Right after World War II, the U.S. Army Corps of Engineers conducted a number of innovative tests on the structural behavior of pavements. In these pioneer studies, heavy vehicles where kept rolling on test tracks until the corresponding pavement sections were severely damaged. The results indicated that pavement lifetime for each given section could be determined in terms of both, the load carried by each axle and the number of load cycles until failure (*1*). The modern procedures for designing sections of pavements and the underlying concepts were established at that time and remain virtually unchanged since then (*2*).

FATIGUE ANALYSIS OF FLEXIBLE PAVEMENTS

Current Spanish Standard 6.1–IC (*3*) quantifies the road traffic volume to be considered at the time of sizing the pavement section by means of the so-called Equivalent Project Traffic (EPT) concept. The EPT is defined as the number of 128 kN equivalent axles that are expected to produce the same damage as all the vehicles rolling on the corresponding lane over the project design life period. According to Kraemer and Albelda (*4*), the EPT can be expressed as

$$E = (\mathrm{ADTh} \cdot 365 \cdot T_p \cdot f) \cdot C \cdot \gamma, \tag{1}$$

where ADTh is the Average Daily Traffic of heavy vehicles (predicted for the year of place in service), T_p is the project design life period (in years), f is a growth factor for the traffic (averaged over the project design life period), C is a conversion coefficient (equivalent 128 kN axles per average heavy vehicle) that depends on the type of pavement and $\gamma \in [1.06, 1.18]$ is a factor of safety for the road traffic volume (as a growing step function of the ADTh value) that is intended to take care of the uncertainty in the values of the loads carried by heavy vehicles. Furthermore, growth factor f can be computed as

$$f = \frac{(1+r)^{T_p} - 1}{rT_p} = 1 + \frac{(T_p - 1)}{2}\, r + \mathscr{O}\left(r^2\right), \tag{2}$$

where r is the estimated annual growth ratio for the road traffic, which is assumed constant over the project design life period.

With regards to Hot Mix Asphalt (HMA) pavements, Standard 6.1–IC (*3*) stipulates the following strain-based fatigue model

$$\varepsilon_r = K \cdot N^{-\alpha} \qquad \Longleftrightarrow \qquad N = (K/\varepsilon_r)^{1/\alpha}, \tag{3}$$

where N is the number of load cycles to failure, which is the maximum number of 128 kN axles that the given pavement section can withstand until the collapse (cracking) occurs. Reference strain ε_r quantifies the structural damage caused by one single load. Specifically, ε_r stands for the maximum horizontal elastic strain at the bottom of the asphalt concrete layer produced by one single static load (128 kN axle) on the given section. On the other hand, K and α are constant coefficients that depend on the HMA type. It seems obvious that the value of reference strain ε_r must be first computed for the further determination of N by means of equation (3).

According to Kraemer and Albelda (*4*), the 128 kN vertical load carried by each axle is supposed to be equally divided among the wheels of each axle. Each wheel is then supposed to deliver its corresponding share of the total vertical load to the pavement within a circular contact

patch. Finally, the corresponding distributed vertical load is supposed to be uniform and equal to the inflation pressure. Therefore, the radius of the contact patch of each wheel is given by

$$a = \sqrt{\frac{V}{\pi\sigma}}, \qquad \text{being} \quad V = \frac{128\ \text{kN}}{n_w}, \tag{4}$$

where V is the share of the total load that corresponds to each wheel, n_w is the number of wheels per axle and σ is the inflation pressure. In the case of axles with two wheels, it seems quite clear that the distance between the wheels allows for neglecting their mutual influence. Therefore, the structural analysis of the pavement reduces to an axisymmetric linear elastic problem in a multi-layered half-space with a vertical pressure σ uniformly distributed within a circle of radius a on the pavement surface. Moreover, reference strain ε_r is identified as the radial strain on the axis of symmetry (see Figure 1). The analytical solution to this problem was first given by Burmister (*5*). In the case of axles with four wheels (which is a more likely condition for a 128 kN load), it seems quite clear that the mutual influence between the twin wheels of each pair cannot be neglected. Therefore, the structural analysis of the pavement no longer reduces to an axisymmetric problem, and reference strain ε_r can no longer be immediately identified. In spite of these difficulties, the analytical solution to this problem can still be (easily, even though not trivially) obtained by adding the two Burmister solutions corresponding to each wheel.

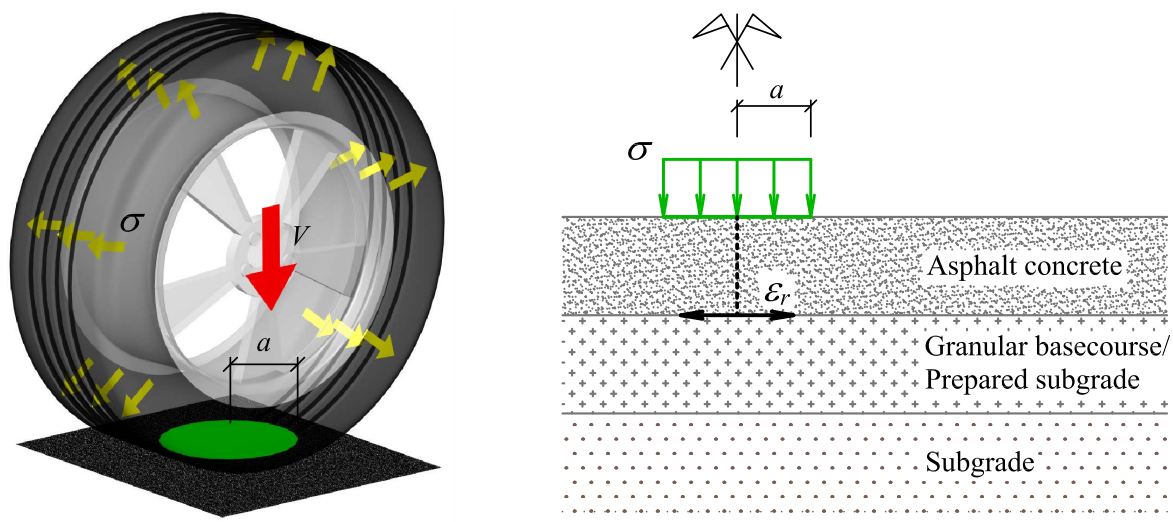

FIGURE 1 Transmission of load to the pavement and reference strain for the fatigue model.

At this point, we recall that the value of E given by (1) represents the number of equivalent 128 kN axles that are expected to roll on the given pavement section over the whole project design life period, while the value of N given by (3) represents the maximum number of 128 kN axles that the given pavement section can withstand until the collapse (cracking) occurs. Therefore, restriction $E \leq N$ must be fulfilled for the pavement section to be technically acceptable.

The above described ideas have their respective counterparts in the standards passed by other road administrations. For instance, the U.S. AASHTO Guide for Design of Pavement Structures (*6*) quantifies the road traffic volume to be considered at the time of sizing the pavement section by means of the so-called Cumulative Equivalent Single Axle Load (CESAL) concept,

which is defined as the number of 80 kN axles that are expected to produce the same damage as all the vehicles rolling on the corresponding lane over the project design life period.

ACCUMULATED DAMAGE AND STRUCTURAL SERVICE LIFE

It seems obvious that fatigue damage increases in a cumulative manner as the number of load cycles grows. However, establishing a precise definition of what we understand for accumulated damage is an open problem (*7*). Going into detail about this topic is out of our scope at this point, since we are mostly interested in assessing the useful life expectancy of a given pavement section rather than the accumulated damage itself (whatever this concept might refer to).

The seminal idea commonly known as the "linear rule" was first introduced by Palmgren as far as 90 years ago. About 20 years later, Miner expressed the same concept in mathematical terms by means of the well known formula

$$\mathscr{D} = \sum_i \left(\frac{n_i}{N_i} \right) \tag{5}$$

which quantifies the total accumulated fatigue damage $\mathscr{D}$ that is reached when different loads are repeatedly applied in different proportions, where n_i stands for the actual number of cycles of each load and N_i stands for the number of cycles to failure when load i is the only one to be applied. As a general rule the system is considered in failure condition when $\mathscr{D} \geq 1$.

Equation (5) implies that the ratio between the actual number of cycles and the number of cycles to failure can be used as an indicator of the accumulated fatigue damage caused by repeated application of one single load level, while these individual indicators can be added if different load levels coexist. These facts provide theoretical support for the equivalent axles concept, which was previously presented.

Following these ideas, an indicator of the accumulated fatigue damage for the fatigue analysis of a HMA pavement section previously presented can be defined as the ratio between E and N, as given by equations (1) and (3) respectively. But the indicator thus defined would only quantify the accumulated fatigue damage at the end of the project design life period T_p. Instead, a more fruitful indicator, as a function of time, will be derived hereafter.

Equations (1) and (2) can be easily modified to give the number of equivalent 128 kN axles over a period of time of length T (in years) starting at the date of place in service as

$$E(T) = (\mathrm{ADTh} \cdot 365 \cdot C \cdot \gamma) \cdot \frac{(1+r)^T - 1}{r} \tag{6}$$

Then, we can define the accumulated fatigue damage indicator

$$\begin{aligned} \psi(\tau) &= \frac{E(T)\big|_{T=\tau T_p}}{N} \\ &= \left(\frac{\mathrm{ADTh} \cdot 365 \cdot C \cdot \gamma}{(K/\varepsilon_r)^{1/\alpha}} \right) \frac{(1+r)^{\tau T_p} - 1}{r}, \qquad \text{being} \quad \tau = T/T_p. \end{aligned} \tag{7}$$

which quantifies the evolution of the accumulated fatigue damage as a function of the time passed since the date of place in service.

Since non dimensional time τ corresponds to real time T scaled in terms of life period T_p, the end of the project design life period is represented by $\tau = 1$. Therefore, the value of $\psi(1)$ indicates if the pavement section can be considered oversize ($\psi(1) < 1$), strictly well sized ($\psi(1) = 1$) or undersized ($\psi(1) > 1$). In the last case, non dimensional time τ_s such that $\psi(\tau_s) = 1$ marks the end of the structural service life at real time $T_s = \tau_s T_p < T_p$.

A largely oversize section is expected to be in good condition far beyond the project design life period, while an undersized section is expected to collapse before the project design life period is over. While the first case can be merely unsatisfactory for economic reasons, the latter will be unacceptable in good engineering practice.

CASE STUDY

Standard 6.1–IC (*3*) includes a catalog with a total of 61 classified sections. The classification system allows for an immediate identification of the suitable sections for each given case, depending on the category of the traffic (as a function of the ADTh) and the structural quality of the subgrade. In spite of this well-meaning approach, a number of members of the Civil Engineering community hold that the mere existence of the catalog may give rise to some perverse consequences. Namely, road design engineers might tend to choose one of the feasible classified sections, rather than working with an optimized design for each given case. In this case, design of many pavement sections would be oversize to a certain extent.

In order to verify this assertion, Kraemer and Albelda presented in 2004 a comprehensive technical evaluation of the whole catalog (*4*). One of the analyzed sections is named T3121 after the traffic category 31 ($100 \leq \text{ADTh} < 200$) and the subgrade structural quality level 2, option 1. This HMA type section is composed of a lower leyer (40 cm thick) of unbound granular material, and an upper layer (16 cm thick) of asphalt concrete. According to the Standard 6.1–IC (*3*), this section is intended for cases in which the ADTh is relatively low and the subgrade structural quality is medium.

In particular, the authors analyzed the behavior of this section for the following data: ADTh $= 171$ heavy vehicles per day, $T_p = 20$ years, $r = 3\%$, $C = 0.5$, $\gamma = 1.12$, $V = 128$ kN$/n_w$, $n_w = 4$, $\sigma = 0.8$ MPa, $K = 6.925 \times 10^{-3}$ and $\alpha = 0.27243$. The value of reference strain ε_r corresponding to this case was obtained by means of the computer program AlizéWin (version 1.02) released in 2002 by the *Laboratoire central des ponts et chaussées* (LCPC), at present *Institut français des sciences et technologies des transports, de l'aménagement et des réseaux* (IFSTTAR). The results given by the authors (*4*) are $E = 0.96 \cdot 10^6$ and $N = 1.5 \cdot 10^6$.

Figure 2 plots the evolution in time of the accumulated fatigue damage indicator (7). Apparently, this section is largely oversize, since the predicted damage at the end of the project design life period is $\psi(1) \approx 0.64 << 1$, and the fatigue failure $\psi(\tau) = 1$ is not reached until $\tau \approx 1.4$, which expands the predicted lifetime for this pavement section 8 years beyond the end of the project design life period.

DYNAMIC AXLE LOADS

As a general rule, current standards define the road traffic volume to be considered at the time of sizing the pavement section in terms of equivalent axles. The value of the load carried by each equivalent axle may differ between different standards (as we have just seen in the cases of the Spanish Standard 6.1–IC and the U.S. AASHTO Guide).

It seems obvious that if a vehicle would roll along a completely straight road, on a perfectly

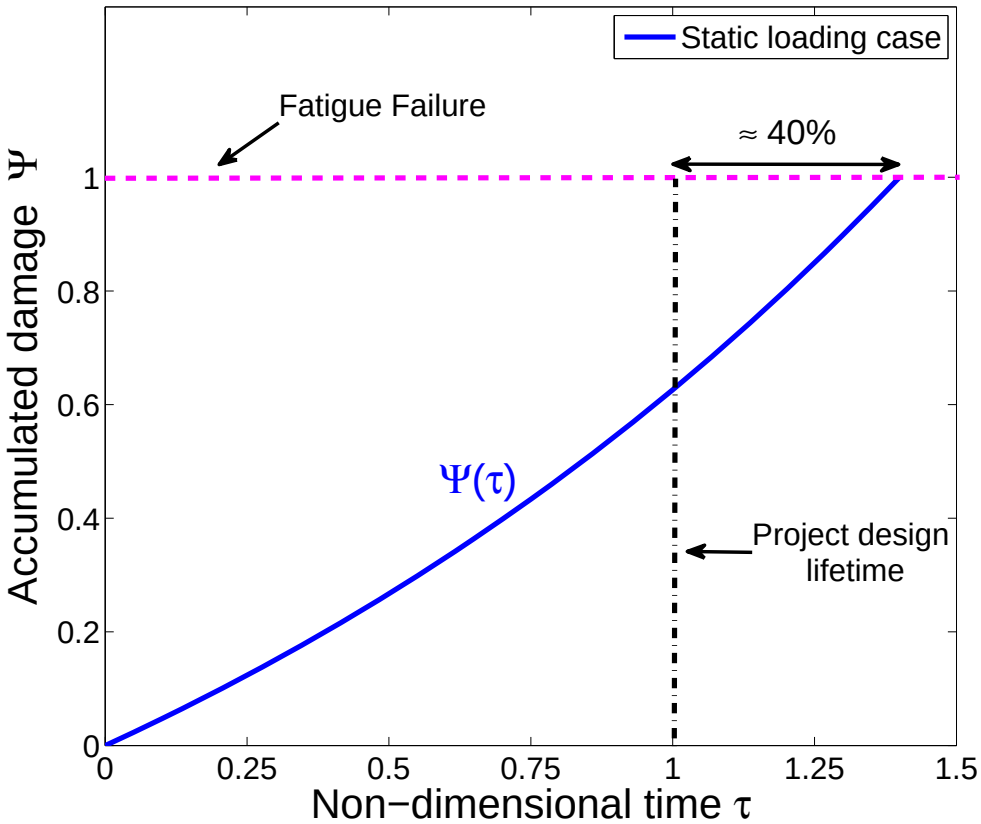

FIGURE 2 Evolution of the accumulated fatigue damage indicator $\psi(\tau)$ for Section T3121.

smooth pavement and at a constant speed, the vertical load carried by each wheel V would be the corresponding share of the total weight, just as it happens when the vehicle is stopped. These are the assumptions which justify expression (4). However, no road surface in the real world is perfectly smooth, which inevitably gives rise to dynamic effects. On the other hand, it seems clear that the peak dynamic load will increase over time, as the roughness of the road surface will do. Therefore, we expect the fatigue damage caused to the pavement by each axle to grow over time, too. In brief, the main objective of this work is to quantify the reduction in the structural service life of the pavement due to the rise of the dynamic axle loads exerted by the traffic, as the progressive deterioration of the road profile occurs.

The idea of taking into account these dynamic effects at the time of sizing the pavement section is not new. As early as in 1986, Cebon (*8*) pointed out that the extra damage caused by dynamic effects is expected to amplify axle loads in successive passes, which could significantly reduce the pavement service lifetime. On the other hand, several contemporary studies showed that peak dynamic loads could easily grow over twice the corresponding static value (*9, 10, 11*). More recently, Shi (*12*) pointed out that dynamic loading is expected to amplify the rate at which damage is caused within the pavement, and Davis (*2*) discussed the need to revise pavement design models in order to take into account dynamic loading, since it could account for a very significant part of the damage suffered by the pavement over its whole service lifetime. Nevertheless, as far as we know, all current standards consider that the load carried by each equivalent axle is invariable

over the whole project design life period. As we have already mentioned, factor of security γ in equation (1) is intended to take care of the uncertainty in the values of the loads carried by heavy vehicles (i.e., the overloading of vehicles above the legal limits). One could argue that this factor could already account for the effects of dynamic loading. However, γ is constant over time and its value is always relatively small, while the peak values of the dynamic loads are expected to grow over time and become much larger than the corresponding static loads. Therefore, we conclude that the mere introduction of this factor of security is not an efficient way of accounting for the effects of dynamic wheel loading.

Let's suppose that the vertical dynamic load carried by each wheel at time T is given by

$$V_d(T) = V\,\Phi(T), \tag{8}$$

where V is the (static) vertical load as considered in expression (4) and $\Phi(T) \geq 1$ is the so-called effective Dynamic Load Amplification (DLA) factor.

Since inflation pressure σ is constant, the radius of the circular contact patch of each wheel carrying this load becomes

$$a_d(T) = a\,\Phi(T)^{1/2}. \tag{9}$$

Therefore, the structural analysis of the pavement still reduces to an axisymmetric elastic problem in a multi-layered half-space with a vertical pressure σ uniformly distributed within a circle of radius $a_d(T)$ on the pavement surface. Again, reference strain $\varepsilon_{rd}(T)$ is identified as the radial strain on the axis of symmetry, and the analytical solution to this problem can be obtained by means of Burmister's expressions (*5*).

For the sake of simplicity, we will assume that

$$\varepsilon_{rd}(T) \approx \varepsilon_r\,\Phi(T). \tag{10}$$

Since we are dealing with a linear elastic problem, stresses and strains are proportional to the external loads. Therefore, the above stated approximation would be exact if the radius of the contact patch of the wheel (a) remained constant while the inflation pressure took the new value $\sigma_d = V_d/(\pi a^2)$. The approximation would also be very accurate if the thickness of the asphalt concrete layer was much larger than the radius of the circular contact patch $a_d(T)$. However, in the case study that we analyze in this paper, the value of the radius of the circular contact patch for the static load is $a \approx 11.28$ cm, which becomes $a_d(T) \approx 15.96$ cm when $\Phi(T) = 2$, while the thickness of the asphalt concrete layer is 16cm and the separation between the twin wheels of each axle is 37.5 cm (*4*). In these conditions, it seems clear that expression (10) can only be considered as a first approximation to the exact value of $\varepsilon_{rd}(T)$. Nevertheless, we expect it to be accurate enough for our purposes at this level.

Then, the number of load cycles to failure corresponding to the dynamic load $V_d(T)$ becomes

$$N_d(T) = \left(K/\varepsilon_{rd}(T)\right)^{1/\alpha} \approx N\,\Phi(T)^{-(1/\alpha)}. \tag{11}$$

On the other hand, we need to derive the dynamic loading counterpart of expression (6). Since $E(T)$ is the number of 128 kN equivalent axles rolling in the time interval $[0,T]$, the number of equivalent axles rolling in the time interval $[T, T+dT]$ will be $E'(T)dT$. Let $E_d(T)$ be the dynamic loading counterpart of $E(T)$, i.e.: the number of 128 kN equivalent axles rolling in the interval $[0,T]$ when the effect of dynamic load (8) is considered. In these terms, $E'_d(T)dT$ will

account for the corresponding number of equivalent axles rolling in the time interval $[T, T+dT]$. In application of Miner's rule (5), the relation between $E(T)$ and $E_d(T)$ can be written as

$$\frac{E'_d(T)\,dT}{N} = \frac{E'(T)\,dT}{N_d(T)} \qquad \Longrightarrow \qquad E'_d(T) = E'(T)\,\frac{N}{N_d(T)} \approx E'(T)\,\Phi(T)^{1/\alpha}. \tag{12}$$

Then, by taking into account expression (6) we can write

$$E_d(T) = \int_0^T E'_d(T)\,dT \approx (\text{ADTh} \cdot 365 \cdot C \cdot \gamma)\,\frac{\ln(1+r)}{r}\,\int_0^T (1+r)^T\,\Phi(T)^{1/\alpha}\,dT. \tag{13}$$

And, finally, the dynamic counterpart of the accumulated fatigue damage indicator (7) can be written as

$$\begin{aligned} \psi_d(\tau) &= \frac{E_d(T)\big|_{T=\tau T_p}}{N} \\ &\approx \psi(\tau)\,\frac{\ln(1+r)}{(1+r)^{\tau T_p}-1}\,\int_{T=0}^{T=\tau T_p} (1+r)^T\,\Phi(T)^{1/\alpha}\,dT, \qquad \text{being } \tau = T/T_p. \end{aligned} \tag{14}$$

LAPLACE TRANSFORM AND TRANSFER FUNCTION

For computing the effective DLA factor $\Phi(T)$ introduced in expression (8), some differential equations must be stated and solved. For this reason, the concepts of Laplace transform and transfer function will be needed from here on.

Given a function $f(t)$ (where t is commonly the time), its Laplace transform $\mathscr{L}\{f(t)\}(s)$ is defined as the function of complex variable $F(s)$ given by the expression

$$\mathscr{L}\{f(t)\}(s) = F(s) = \int_{t=0}^{t=\infty} e^{-st} f(t)\,dt, \qquad \text{where} \quad s \in \mathbb{C}. \tag{15}$$

The Laplace Transform is a linear operator. Therefore, for arbitrary constants a and b it verifies

$$\mathscr{L}\{a\,f(t) + b\,g(t)\}(s) = a\,\mathscr{L}\{f(t)\}(s) + b\,\mathscr{L}\{g(t)\}(s). \tag{16}$$

It can also be easily proven that the transform of the n-th derivative of a function $f(t)$ satisfies

$$\mathscr{L}\left\{f^{(n)}(t)\right\}(s) = s^n\,\mathscr{L}\{f(t)\}(s) - \sum_{i=1}^{n} s^{n-i}\,f^{(i-1)}(0). \tag{17}$$

Should the Laplace transform $F(s)$ be known, the original function $f(t)$ can be reconstructed from this information. A (non trivial) procedure is given by the expression

$$\mathscr{L}^{-1}\{F(s)\}(t) = f(t) = \frac{1}{2\pi i}\,\int_{\chi-\infty i}^{\chi+\infty i} e^{st}\,F(s)\,ds, \tag{18}$$

where integration is performed in the complex plane over the vertical line $\text{Re}(s) = \chi$, being χ larger than the real part of all the singularities of $F(s)$. In these terms, it is said that the real function $f(t)$ is the inverse Laplace transform of the complex variable function $F(s)$.

As a general rule, the Laplace transform can be used for solving differential and integral equations by means of analytical techniques. Essentially, the procedure consists in calculating the transform of the equation, clearing up the transform of the solution and performing the inverse transformation, which gives the solution to the original problem. Besides its utility for solving mathematical problems, expression (18) shows that the Laplace transform $F(s)$ quantifies the so-called spectrum of function $f(t)$, which is the contribution of each complex frequency s to the actual value of $f(t)$. For this reason, when the Laplace transform $F(s)$ is obtained, it is said that the spectral analysis of function $f(t)$ is being performed. It is also said that this operation turns the study in the domain of time (t), into the study in the domain of frequency (s).

Given two functions, $f(t)$ and $g(t)$, the so-called transfer function of the first ($f(t)$) with respect to the second ($g(t)$) is defined as the quotient of their Laplace transforms

$$H_{fg}(s) = \frac{\mathscr{L}\{f(t)\}(s)}{\mathscr{L}\{g(t)\}(s)}. \tag{19}$$

As it is obvious, the transfer function quantifies how much the second function contributes to the spectrum of the first.

QUARTER-VEHICLE MODEL

In the late 1970s the World Bank required a number of road roughness measures to be performed in order to run a cost model on the projects being financed. At that time, roughness measures could be very different depending on the procedure being used. To solve this problem, the World Bank organized the International Road Roughness Experiment (IRRE) in 1982 in Brazil. The main objective of this conference was the definition of a standard roughness measurement technique to be used thereafter in the quality control of the projects financed by the World Bank. Among the different roughness indices that were proposed, the inches/mile rate computed by means of the Quarter-Car (QC) model —previously defined by Gillespie et al. in the NCHRP Report 228 (*13*)— was considered the most appropriate. As a result of these agreements, the World Bank defined the so-called International Roughness Index (IRI) as a new standard in 1986 (*14, 15*). Currently, the IRI is the most widespread, worldwide used index for evaluating the roughness of a road.

The IRI is intended to account for the accumulated vertical displacements which are experienced by the body of a regular car due to the roughness of the road surface. To quantify this effect, the dynamic behavior of a standardize car must be simulated. This is what the QC model is stated for. On the other hand, the effective DLA factor $\Phi(T)$ introduced in expression (8), is intended to account for the rise in the vertical load carried by each wheel of a regular heavy vehicle due to the progressive deterioration of the road surface. To quantify this effect, the dynamic behavior of a standardize heavy vehicle must be simulated by means of a suitable mathematical model. The Quarter-Vehicle (QV) model presented below, is an extension on the QC concept and allows for computing both, the IRI and factor $\Phi(T)$, provided that the appropriate values of the model parameters were used for each case.

The QV model is shown in Figure 3. Essentially, the suspended body of the quarter-vehicle is represented by the sprung mass m_2, which is linked to the axle by the suspension. The suspension response to deformation is modeled in terms of the spring with elastic constant k_2 and the damper with damping coefficient c_2. The corresponding half-axle is represented by the unsprung mass m_1, which is linked to the pavement by the only wheel. The tire response to deformation is modeled in terms of the spring with elastic constant k_1 and the damper with damping coefficient c_1. The

value $c_1 = 0$ Ns/m must be taken for the IRI calculations. This implies that wheel damping is considered negligible at this level. Nevertheless, wheel damping cannot be neglected in the case of heavy vehicles, which justifies the need for including coefficient c_1 in the QV model. The contact between the wheel and the road surface is supposed to be reduced to a single point.

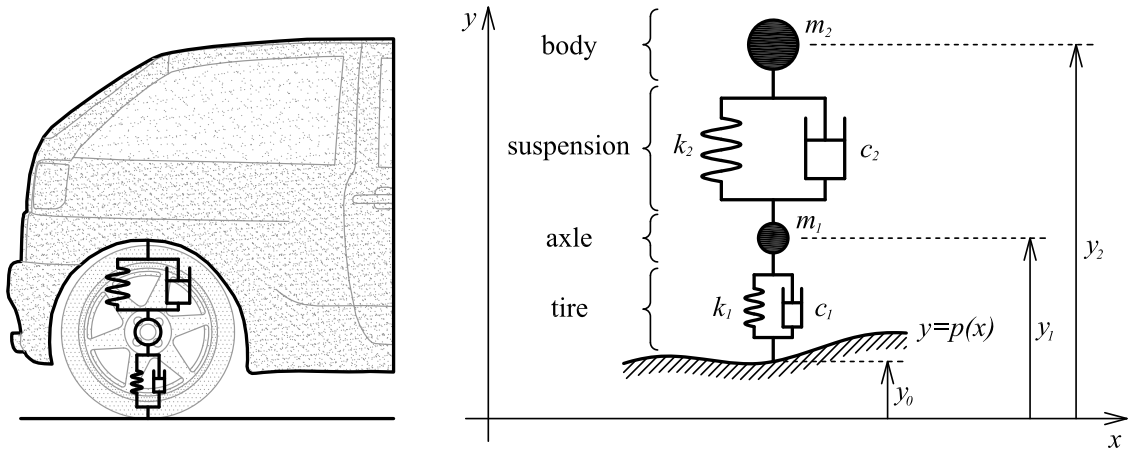

FIGURE 3 Quarter-Vehicle (QV) Model.

The road profile to be followed by the wheel, is represented by a suitable function $y = p(x)$ for $x \geq 0$, such that $p(0) = p'(0) = 0$. In addition, the QV is set to roll at a constant horizontal speed v and the virtual ride starts in the position $x = 0$ at (local) time $t = 0$. Therefore, $y_0(t) = p(x)\big|_{x=vt}$ and the dynamic system has two degrees of freedom, namely: the unknown functions $y_1(t)$ and $y_2(t)$. As initial conditions (compatible with the IRI calculation), we take $y_1(0) = \dot{y}_1(0) = 0$, $y_2(0) = \dot{y}_2(0) = 0$.

By applying Newton's second law to both, the unsprung and the sprung masses, we get the system of ordinary differential equations

$$\underset{\sim}{M}\,\ddot{\bar{u}}(t) + \underset{\sim}{C}\,\dot{\bar{u}}(t) + \underset{\sim}{K}\bar{u}(t) = \bar{b}\,\ddot{y}_0(t), \tag{20}$$

in terms of the new vectorial variable $\bar{u}(t)$, where

$$\underset{\sim}{M} = \begin{bmatrix} (m_1+m_2) & m_2 \\ m_2 & m_2 \end{bmatrix}, \quad \underset{\sim}{C} = \begin{bmatrix} c_1 & 0 \\ 0 & c_2 \end{bmatrix}, \quad \underset{\sim}{K} = \begin{bmatrix} k_1 & 0 \\ 0 & k_2 \end{bmatrix}, \quad \bar{b} = -\begin{Bmatrix} (m_1+m_2) \\ m_2 \end{Bmatrix}, \tag{21}$$

and

$$\bar{u}(t) = \begin{Bmatrix} u_1(t) \\ u_2(t) \end{Bmatrix}, \qquad u_1(t) = y_1(t) - y_0(t) - \delta_1, \qquad u_2(t) = y_2(t) - y_1(t) - \delta_2, \tag{22}$$

being δ_1 and δ_2 the static values of $(y_1 - y_0)$ and $(y_2 - y_1)$ when the vehicle is stopped. The actual unknowns $\bar{u}(t)$, as defined in (22), represent the oscillations of the unsprung and the sprung masses with respect to their respective equilibrium positions when the vehicle is stopped at each given point $x = vt$.

On the other hand, the dynamic vertical load $V_d(t)$ exerted by the wheel on the pavement along the ride can be computed as

$$V_d(t) = V\,\big(1 + \eta(t)\big), \quad \text{for } V = (m_1+m_2)g, \;\; \eta(t) = \frac{-1}{(m_1+m_2)g}\,\big(c_1\,\dot{u}_1(t) + k_1\,u_1(t)\big). \tag{23}$$

in terms of the static vertical load V and the dynamic amplification function $\eta(t) \geq -1$. If function $\eta(t)$ gets to decrease as to reach its lower bound, the wheel could take off from the road surface. If this situation occurs, the model needs to be adjusted in order to track the behavior of the system during the flight, until the wheel lands on the pavement again.

By applying the Laplace transform properties to these equations we can write the transfer function of the unknown $\bar{u}(t)$ with respect to $y_0(t)$ as

$$H_{\bar{u}\,y_0}(s) = \left[\underset{\sim}{M}\, s^2 + \underset{\sim}{C}\, s + \underset{\sim}{K}\right]^{-1} \; \bar{b}\, s^2, \tag{24}$$

and the transfer function of the unknown $\eta(t)$ with respect to $u_1(t)$ as

$$H_{\eta\, u_1}(s) = \frac{-1}{(m_1+m_2)g}\, \left(c_1\, s + k_1\right). \tag{25}$$

In these terms, the Laplace transforms of the unknown functions $\bar{u}(t)$ and $\eta(t)$ can be written as

$$\mathscr{L}\left\{\bar{u}(t)\right\}(s) = H_{\bar{u}\,y_0}(s)\;\; \mathscr{L}\left\{y_0(t)\right\}(s), \qquad \mathscr{L}\left\{\eta(t)\right\}(s) = H_{\eta\, y_0}(s)\;\; \mathscr{L}\left\{y_0(t)\right\}(s), \tag{26}$$

and the Laplace transform of $y_0(t)$ can be given in terms of the Laplace transform of the road profile $p(x)$ as

$$\mathscr{L}\left\{y_0(t)\right\}(s) = \frac{1}{v}\, P(\xi)\big|_{\xi=s/v}, \qquad \text{being} \quad P(\xi) = \mathscr{L}\left\{p(x)\right\}(\xi) = \int_{x=0}^{x=\infty} e^{-\xi x} p(x)\, dx. \tag{27}$$

Finally, the use of the inverse Laplace transform allows for solving the dynamic problem in a formal manner.

The above stated mathematical model can be discretized on the basis of the Discrete Fourier Transform (DFT) concept (*16*).

QUANTIFYING THE IRI AND THE EFFECTIVE DLA FACTOR

For the IRI calculation, the QV parameters must be adjusted to those of the standard QC model as defined in (*13*). These are shown in column QC-IRI of Table 1. During the simulation, the quarter-vehicle is set to roll at speed $v = 80$ km/h along a stretch of length $L = 100$ m. Hence, the total time needed to complete the virtual ride is $t_{\max} = L/v = 4.5$ s.

TABLE 1 Standard Values of the Parameters for several Quarter-Vehicle Models.

Param.	Units	**QC–IRI**	**QHV–LS**	**QHV–AS**	**QHV–WB**
m_2	kg	250	6,700	8,900	6,600
k_2	N/m	15,825	4,000,000	2,000,000	4,000,000
c_2	Ns/m	1,500	80,000	40,000	80,000
m_1	kg	37.5	500	1,100	1,100
k_1	N/m	163,250	3,500,000	3,500,000	3,500,000
c_1	Ns/m	0	4,000	4,000	4,000

The profile function $y = p(x)$ must be derived from in situ measures gathered by a suitable device (the so-called profiler). A moving average low-pass filter with a 250-mm base length must be applied to the raw profile (if not previously done by the profiler) before performing the simulation. The rationale for the use of this filter is the need to remove the highest frequency components of the roughness, which combined effects are expected to be negligible due to the compliance of the tire section in contact with the pavement (*17*).

Once the results of the simulation are known, the IRI can be computed as

$$\mathrm{IRI} = \frac{1}{L} \int_{t=0}^{t=t_{\max}} |\dot{u}_2| \, dt. \tag{28}$$

For quantifying the effective DLA factor $\Phi(T)$, the QV parameters must be adjusted as to fit the characteristics of a suitable Quarter-Heavy Vehicle (QHV) model. Columns QHV–LS, QHV–AS and QHV–WB of Table 1 show the corresponding values for three possible QHV models with different types of suspension, namely: Leaf Spring (*18*), Air Spring (*1*) and Walking Beam (*18*), respectively. At present, there are no regulations to be followed on this subject, nor with regards to the speed v and the stretch length L to be considered in the simulations. In the example presented in this paper, the selected parameters correspond to a heavy vehicle with air spring suspension, as shown in column QHV–AS of Table 1, while v, L and $t_{\max}$ were kept as in the IRI case.

At this point, we highlight the distinction between global time T (in years, measured from the date of place in service) that is used to track the condition of the road along its life time, and local time t (very likely in seconds, starting at the moment T in which the QV simulation is initiated) that is used to track the dynamic response of the QV model along a short interval of time (4.5 s).

Taking $\Phi(T) = \big(1+\eta(t)\big)$ in expressions (8), (9), (10) and (11), we conclude in application of Miner's rule that the damage caused by a single equivalent axle at time t right under the actual position of the wheel ($x = vt$) is (approximately) proportional to $(1+\eta(t))^{1/\alpha}$. Since the damage is different at each point $x \in [0, L]$, the averaged damage in the stretch could be considered as a reasonable value for the damage associated to the effective DLA factor, which gives the expression

$$\Phi(T)^{1/\alpha} \approx \frac{1}{t_{\max}} \int_{t=0}^{t=t_{\max}} \big(1+\eta(t)\big)^{1/\alpha} \, dt. \tag{29}$$

EVOLUTIONARY MODEL FOR THE ACCUMULATED DAMAGE

Let $p(x)$ represent the road profile at (global) time T. Equations (20)–(27) provide the way to get the dynamic amplification function $\eta(t)$ which corresponds to the actual condition of the road. This information can be immediately used to get the actual value of the effective DLA factor $\Phi(T)$ by means of expression (29).

Therefore, if factor $\Phi(T)$ was known for all T, equation (13) could be used to get the number of 128 kN equivalent axles considering dynamic loads $E_d(T)$ at any time T. In this terms, equation (14) would automatically provide the time evolution of the dynamic accumulated fatigue indicator $\psi_d(\tau)$, which is the main objective of this work.

However, the model presented up to this moment is not fully operational, since it contains no tools to predict the time evolution of the road profile. To make the model complete, we need to cast light on how the road profile deteriorates over time.

According to Paterson (*19, 20*) the time evolution of the IRI can be described by the expression

$$\mathrm{IRI}(T) = 1.04 \cdot e^{\beta T} \cdot \mathrm{IRI}_0 + 2.63 \cdot 10^{-4} \cdot (1+\mathrm{SNC})^{-5} \cdot \mathrm{CESAL}(T), \tag{30}$$

where IRI_0 is the initial value of the IRI at the date of place in service; β is a coefficient in the range $[0.01, 0.70]$ which depends on the local climatic conditions; SNC is a parameter which quantifies the structural quality of the road as defined in (*6*); and $\mathrm{CESAL}(T)$ is the accumulated traffic at time T expressed as the number of 80 kN equivalent axles. In application of Miner's rule, taking into account that the fatigue model being used is given by equation (3), and making the usual simplifications for converting equivalent axles, the value of $\mathrm{CESAL}(T)$ can be expressed in terms of $E(T)$ as

$$\mathrm{CESAL}(T) \approx E(T) \cdot \left(\frac{128}{80}\right)^{1/\alpha}. \tag{31}$$

As shown in expression (27), the road profile $p(x)$ is introduced in the dynamic model by means of its Laplace transform $P(\xi)$, that can be expressed in polar form as

$$P(\xi) = \left|P(\xi)\right| \, e^{\,i \, \arg(P(\xi))}. \tag{32}$$

The modulus of the Laplace transform can be written in terms of the so-called Power Spectral Density (PSD) function $\varphi(\omega)$ as

$$\left|P(\xi)\right| = \left(\varphi(\omega)\big|_{\omega=-i\xi}\right)^{1/2}. \tag{33}$$

In (*21, 22*), the following general expression is suggested for the PSD function of the pavement

$$\varphi(\omega) = \varphi(\omega_0)\left(\frac{\omega}{\omega_0}\right)^{-n}. \tag{34}$$

where n is a real constant in the range $[2,3]$ and $\omega_0 =$ is a cutting upper limit for ω. According to Cebon (*1*), the above expression is appropriate for this case. In this work, we take $n = 2$ and $\omega_0 = 0.1$ m^{-1}. On the other hand, $\varphi(\omega_0)$ is the maximum value of the PSD of the profile, which grows concurrently with the deterioration of the road surface. According to Misaghi (*18*), the value of $\varphi(\omega_0)$ can be expressed in terms of the IRI at time T as

$$\varphi(\omega_0) = 2.52 \cdot 10^{-6} \cdot \left(\mathrm{IRI}(T)\right)^{2.37}. \tag{35}$$

On the other hand, it is accepted that the argument of the Laplace transform $P(\xi)$ is not relevant in this case, which allows for taking $\arg(P(\xi)) \approx 2\pi\,\mathrm{rand}()$, being rand() any suitable function giving uniformly distributed numbers in the interval $[0,1]$.

APPLICATION EXAMPLE

Figure 4 plots the evolution in time of the accumulated fatigue damage indicator (14), computed by means of this model, for the previously studied Section T3121. With regards to equation (30) for the time evolution of the IRI, the values $\beta = 0.15$ and $\mathrm{SNC} = 4.5$ were used in this work. This value of coefficient β can be considered suitable for roads in this region of Spain (Galicia)

according to the opinion of several experts in the field, both from the Road Department and from *Eurovia* (one of the main contractors for road construction and maintenance operations in Europe, which is the corporation that primarily supported this research). On the other hand, the value of parameter SNC is the result given by the procedure described in the AASHTO Guide (*6*) for the section being considered.

It is obvious that this section is not oversize (as the Standard 6.1–IC predicts) but largely undersized. We highlight that the fatigue failure $\psi(\tau_s) = 1$ is reached for $\tau_s \approx 0.6$, which shrinks the structural service lifetime to about 12 years, 8 years less than the project design life period and 16 years less than the prediction given by the Standard.

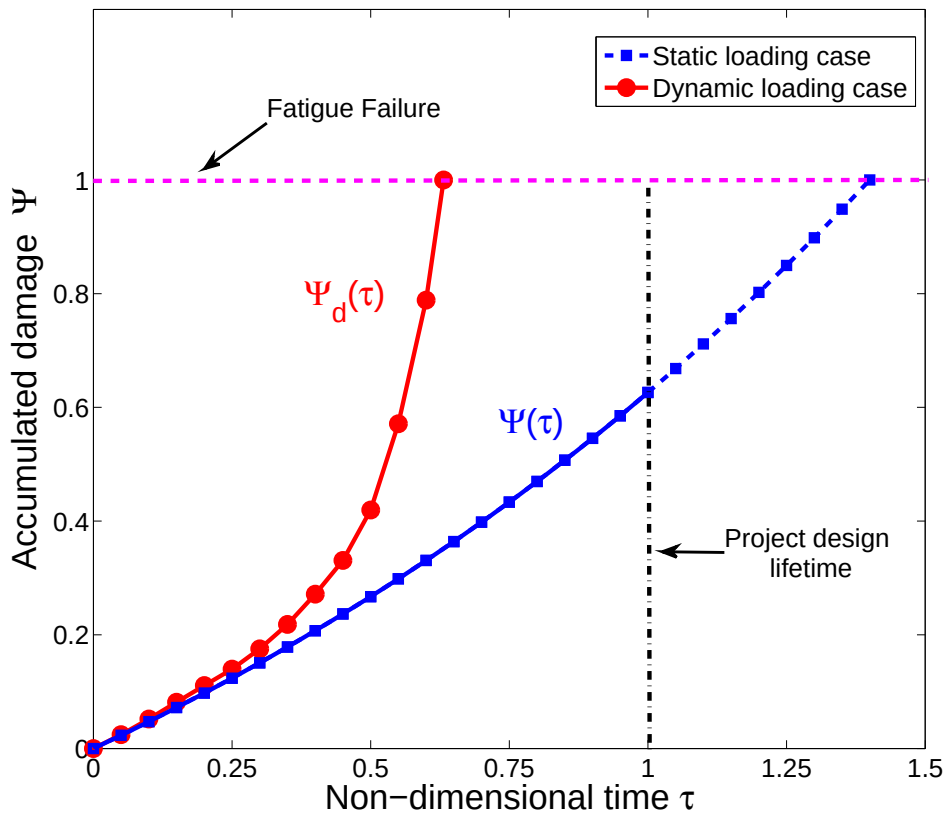

FIGURE 4 Evolution of the accumulated fatigue damage indicator $\psi_d(\tau)$ for Section T3121.

Further examples and a discussion on the application of this model for predicting the structural service life under different conservation strategies will be presented in forthcoming papers.

CONCLUSIONS

In this paper, a comprehensive model for the fatigue analysis of flexible pavements considering the effects of dynamic axle loads has been presented. The implementation of the model herein presented is specific for the Spanish Standard 6.1–IC, but the underlying concepts are not restrictive and can be applied to any strain-based fatigue law. Therefore, the model can be easily adapted to fit the distinctive features of other regulations. The model has been implemented and one application example has been presented.

As it has been shown, taking into account the dynamic axle load in the fatigue analysis of a flexible pavement may lead to a dramatic fall in the predicted structural service life. The importance of this assertion is evident, which calls for considering the possibility of including these effects in future revisions of the current Standards.

ACKNOWLEDGMENTS

This work has been primarily supported by *Holding Eurovía España* by means of a research contract awarded by its subsidiary firm *OVISA Pavimentos y Obras S.A.* to the *Fundación de la Ingeniería Civil de Galicia*.

Partial support has also been provided by FEDER funds of the European Union, Grant #DPI2012-33622 of the *Ministerio de Economía y Competitividad* of the Spanish Government, Grant #CN2011/002 of the *Consellería de Educación e Ordenación Universitaria* of the *Xunta de Galicia*, and Research fellowships of the *Universidad de A Coruña*.

The authors are grateful for useful advice and suggestions from Gerardo Pallares (Civil Engineer, MSc), Head of Road Department at the *Axencia Galega de Infraestructuras*, and Gonzalo Vázquez (Civil Engineer), co-director of the contract for the maintenance of 1,600 km of the Galician road network.

REFERENCES

1. Cebon, D. *Handbook of Vehicle-Road Interaction*. Swets & Zeirlinger Eds., Lisse (Netherlands), 1999.
2. Davis, L.E. Dynamic Wheel Loads from Heavy Vehicles. *Queensland Roads*, Issue 9, 2010, pp. 16–27.
3. Dirección General de Carreteras, Secretaría de Estado de Infraestructuras. *Norma 6.1–IC "Secciones de Firme" de la Instrucción de Carreteras*. Orden FOM/3460/2003 de 28 de noviembre (BOE de 12 de diciembre de 2003). Centro de Publicaciones del Ministerio de Fomento, Gobierno de España, 2003.
4. Kraemer, C., and R. Albelda. Evaluación técnico-económica de las secciones de firme de la Norma 6.1–IC. In *VI Congreso Nacional de Firmes: Normalización e Innovación*, Asociación Española de la Carretera, Madrid, 2004. http://www.aecarretera.com/congresos/PO_04.pdf. Accessed Nov. 14, 2014.
5. Burmister, D. M. The general theory of stresses and displacements in layered systems. *Journal of Applied Physics*, Vol. 16, 1945, pp. 89-–94.
6. American Association of State Highway and Transportation Officials. *AASHTO Guide for Design of Pavement Structures 1998*. AASHTO, Washington, 1998.
7. Fatemi, A., and L. Yang. Cumulative fatigue damage and life prediction theories: a survey of the state of the art for homogeneous materials. *International Journal of Fatigue*, Vol. 20, No. 1, 1998, pp. 9—34.
8. Cebon, D. Road Damaging Effects of Dynamic Axle Loads. In *9th International Symposium on Heavy Vehicles Weights and Dimensions*, Kelowna (Canada), 1986.
9. Woodrooffe, J.H.F., P.A. LeBlanc, and K.R. LePiane. Effects of suspension variations on the dynamic wheel loads of a heavy articulated highway vehicle. In *Vehicle Weights and Dimensions Study*, Vol. 11, Canada, 1986.
10. Woodrooffe, J.H.F., and P.A. LeBlanc. The Influence of Suspension Variations on Dynamic

Wheel Loads of heavy Vehicles. In *Society of Automotive Engineers*, Paper No. 861973, 1986.

11. Cole, D.J., and D. Cebon. Simulation and measurement of dynamic tyre forces. In *Second International Symposium on Heavy Vehicle Weights and Dimensions*, Kelowna (Canada), 1989.
12. Shi, X.M., and C.S. Cai. Simulation of Dynamic Effects of Vehicles on Pavement Using a 3D Interaction Model. *Journal of Transportation Engineering*, Vol. 135, 2009, pp. 736–744.
13. Gillespie, T.D., M.W. Sayers, and L. Segel. *Calibration of Response-Type Road Roughness Measuring Systems, National Cooperative Highway Research Program Report No. 228*. Transportation Research Board of the National Academies, Washington, D.C., 1980.
14. Sayers, M.W., T.D. Gillespie, and C.A.V. Queiroz. *The International Road Roughness Experiment: Establishing Correlation and Calibration Standard for Measurement*. The World Bank, Technical Paper No. 45, Washington, D.C., 1986.
15. Sayers, M.W., T.D. Gillespie, and W.D.O. Paterson. *Guidelines for the Conduct and Calibration of Road Roughness Measurements*. The World Bank, Technical Paper No. 46, Washington, D.C., 1986.
16. Melis, M. *Dinámica Vertical de la Vía*. Cátedra de Ferrocarriles, Universidad Politécnica de Madrid, Madrid (Spain), 2008.
17. Sayers, M. W., and S.M. Karamihas. *The Little Book of Profiling*. The Regent of the University of Michigan, Michigan, 1998.
18. Misaghi, S. *Impact of Truck Suspension and Road Roughness on Loads Exerted to Pavements*. MSc Thesis Dissertation, University of Texas at El Paso. ETD Collection for UTEP, Paper AAI1494314, El Paso, 2011.
19. Paterson, W.D.O. International Roughness Index: Relationship to Other Measures of Roughness and Riding Quality. In *Transportation Research Record: Journal of the Transportation Research Board, No. 1084*, Transportation Research Board of the National Academies, Washington, D.C., 1986, pp. 49-59.
20. Zhang, W. *Fatigue Performance of Existing Bridges under Dynamic Loads from Winds and Vehicles*. PhD Thesis Dissertation, Louisiana State University, Baton Rouge, 2012. http://etd.lsu.edu/docs/available/etd-04042012-211349/unrestricted/zhang_diss.pdf. Accessed Nov. 14, 2014.
21. International Organization for Standardization. *Proposals for generalised road inputs to vehicles*. ISO/TC/108/WGp draft No. 3e, ISO, 1972.
22. Zhang, W., C.S. Cai, and F. Pan. Nonlinear fatigue damage assessment of existing bridges considering progressively deteriorated roads conditions. *Engineering Structures*, Vol. 56, 2013, pp. 1922–1932.